Marinetto, E., Garcia-Mato, D., Garcia, A., Martinez, S., Desco, M. & Pascau, J. (2018). Multicamera Optical Tracker Assessment for Computer Aided Surgery Applications. *IEEE Access,* vol. 6, pp. 64359–64370.

DOI: 10.1109/access.2018.2878323

IEEE Access
Multidisciplinary | Rapid Review | Open Access Journal

Multicamera Optical Tracker Assessment for Computer Aided Surgery Applications

Eugenio Marinetto[1,2], David García-Mato[1,2], Alonso García[1], Santiago Martínez[3], Manuel Desco[1,2,4], Javier Pascau[1,2]

[1]Departamento de Bioingeniería e Ingeniería Aeroespacial, Universidad Carlos III de Madrid, 28911 Leganés, Madrid, Spain
[2]Instituto de Investigación Sanitaria Gregorio Marañón, Madrid, Spain
[3]RoboticsLab, Universidad Carlos III de Madrid, 28911 Leganés, Madrid, Spain
[4]Centro Nacional de Investigaciones Cardiovasculares Carlos III (CNIC), Madrid, Spain

Corresponding author: Javier Pascau (e-mail: jpascau@ing.uc3m.es).

Supported by projects TEC2013-48251-C2-1-R, PI15/02121, PI18/01625 (Ministerio de Economía y Competitividad, Instituto de Salud Carlos III and European Regional Development Fund "Una manera de hacer Europa") and TOPUS-CM S2013/MIT-3024 (Comunidad de Madrid).

ABSTRACT Image-guided interventions enable the surgeon to display the position of instruments and devices with respect to the patient's imaging studies during surgery by means of a tracker device. Optical trackers are commonly chosen for many surgical applications when high accuracy and robustness are required. OptiTrack is a multicamera optical tracker whose number of sensors and their spatial configuration can be adapted to the application requirements, making it suitable for surgical settings. Nonetheless, no extensive studies of its accuracy are available. The purpose of this study was to evaluate an 8-camera optical tracker in terms of accuracy, miscalibration sensitivity, camera occlusions and tool detection in a feasible clinical setup. We studied the tracking accuracy of the system using a robotic arm (~μm precision) as the gold standard, a single reflective marker and various tracked objects while the system was installed in an operating room. Miscalibration sensitivity was 0.16 degrees. Mean target error was 0.24 mm for a single marker, decreasing to 0.05 mm for tracked tools. Single-marker error increased up to 1.65 mm when 5 cameras where occluded, although 75% of the working volume showed an error lower than 0.23 mm. The accuracy was sufficient for navigating the collimator in intraoperative electron radiation therapy, improving redundancy and allowing large working volumes. The tracker assessment we present and the validated miscalibration protocol are important contributions to image-guided surgery, where the choice of the tracker is critical and the knowledge of the accuracy in situations of camera occlusion is mandatory during surgical navigation.

INDEX TERMS Computer aided interventions, infrared tracking, multicamera optical tracker, optical tracking

I. INTRODUCTION

Image-guided interventions (or image-guided surgery, IGS) are medical procedures in which surgeons are able to observe the position of surgical tools and therapeutic devices with respect to the patient's image studies. IGS has been implemented in neurosurgery, orthopedic surgery, cardiovascular surgery, and radiation oncology applications, with the aim of improving the performance, speed and safety of surgical procedures [1], [2]. One of the main components of IGS is the tracker device which is needed to obtain the position of the tools and patient during the surgical procedure. An accurate correlation of the pre-operative imaging to the operative field is of special importance in IGS [3], [4]. IGS solutions enhance the surgical experience providing free-hand navigation, positioning of equipment or guidance for a mechatronic system.

Trackers are commonly classified as mechanical, magnetic or optical. Optical trackers use cameras surrounding the working area to determine the position of tools through various visualization techniques. As a limitation, they need a clear line-of-sight between the tracked object and the cameras, which is not always possible, e.g. when tools such as catheters and probes are tracked inside the patient's anatomy. In such situations, electromagnetic trackers are better suited [1], [5]. Nevertheless, optical trackers are still preferred for many surgical applications since they show higher accuracy and larger working volumes than mechanical and magnetic trackers [2], [6]–[8].

Examples of commercially available optical trackers for IGS include fusionTrack (Atracsys Inc., Puidoux, Switzerland) and Polaris (NDI Inc., Ontario, Canada). These systems are based on infrared cameras and calculate the position of passive retro-reflective markers, which are small spheres coated with IR reflective material. Tracking is based on the projection (Fig. 1, a5) of the markers into each camera plane (Fig. 1, a4). However, the relative position of each camera in the space and the optical lens parameters (e.g. focal length, optical aberrations) need to be known in advance to compute the three-dimensional position of markers by forward projection [9]. This set of parameters is commonly estimated through prior calibration.

Once calibration parameters are known, the system estimates the three-dimensional location of a marker as the intersection of the rays coming from each camera projection plane. In the same manner, the expected projection on each camera plane (Fig. 1, a3) can be computed from the marker's three-dimensional position (Fig. 1, a2) and the calibration parameters. Ideally, the actual projection (Fig. 1, a5) will match the expected projection (Fig. 1, a3) and all projection rays will collide at the true three-dimensional location of the marker (Fig. 1, a2). However, this is not true under non-ideal conditions (due to miscalibration). The absolute difference between expected and actual projections in each camera plane is known as *projection error* (Fig. 1, a6). The difference between the estimated (Fig. 1, a7) and the true three-dimensional location of the marker (Fig. 1, a2) is defined as *tracking error* (Fig. 1, a8). The *tracking error* is a main figure of merit during the trackers assessment for IGS [1], [10]–[12].

During the calibration process the system collects the synchronized projections of a group of reflective markers that are arranged in a unique geometry which is called rigid-body. The simplest rigid-body is composed of at least three reflective markers. Distances and angles between the markers are fixed (rigid) with respect to each other. Usually, a calibration algorithm minimizes the *projection* and/or the *tracking error* in an iterative scheme to estimate the calibration parameters. After successful calibration, the *projection error* (Fig. 1, a6) is expected to be sufficiently small, and the system is ready to track rigid-bodies -which are attached to the tools of interest- and to estimate their position and orientation inside the working volume. However, when a miscalibration occurs (for one or more cameras), the *projection error* and the *tracking error* increase.

Both fusionTrack and Polaris systems must work under occlusion-free conditions since they share the common constraint of using a single pair of tracking cameras [7], [13], [14]. If any of the two cameras is occluded, the system is no longer able to determine the three-dimensional position of any marker. Optical trackers formed by more than two cameras (hereinafter referred to as multicamera systems) lead to data redundancy and benefit a clear line-of-sight, thus enabling the system to overcome this limitation. However, to our knowledge, there are no commercial multicamera trackers offering tracking for surgical applications [6], [13], [15].

OptiTrack [16] is a commercial multicamera optical tracker in which the number of cameras and their spatial configuration are flexible (i.e., they can be modified depending on the application requirements) in contrast to two-camera systems. This feature could make it more versatile for tracking different environments, such as a complete operating room (OR), with almost no restrictions on the working volume. The main advantages of this system are the tracking accuracy (submillimeter level, according to the manufacturer) and its robustness against camera occlusions. Consequently, it is better suited for environments that are prone to occlusions. OptiTrack has been used for tracking purposes in several fields [17]–[20]. Nevertheless, few studies have examined the use of multicamera trackers during IGS [6], [7], [21]–[25].

We previously presented a navigation system for intraoperative electron radiation therapy procedures (IOERT) based on OptiTrack. The feasibility of this navigation workflow for the clinical environment was demonstrated [6], [26]. We evaluated the system accuracy when locating the IOERT radiation collimator. In IOERT procedures, static accuracy is the main point of interest, and dynamic accuracy (real-time tracking) is not a key issue.

When a navigation system is evaluated for IGS, the principal concern is the *accuracy* of the system which determines its clinical applicability, functionality and safety [1], [3], [4], [10], [11], [27]. We will evaluate the accuracy of a tracker as the difference between the tracker's measured and true position (*trueness*) due to the *intrinsic* (technical) limitations.

Several error sources can affect the correct three-dimensional location of surgical tools over patient images [3], [12]. Common factors that affect the accuracy of IGS navigation include image-to-world registration outcome [3], [28], [29], the technical specifications of the tracking cameras, a non-optimal design of rigid bodies [4], [30]–[32], and the distance between the markers and the sensors [11], [32]. Multicamera optical trackers, in particular, are also dependent on the calibration process [3], [8], [32], [33]. Some of these factors have been studied in order to evaluate the feasibility of different trackers for IGS applications [3], [7], [8], [10], [33]–[35]. However, most studies have focused on a specific IGS application of interest [4], [5], [11], [32], [36]–[38]. Hence, it is difficult to extrapolate their results to other applications or compare the accuracy of different commercial systems [11].

A common limitation of some of the previously reported assessments is the use of another tracker as the gold standard for the accuracy evaluation. Those studies assume that the chosen gold standard is sufficiently accurate [5], [8], [37], [39] which may not be true. Although the cited studies

provide valuable information, a true gold standard is needed for persuasive evaluation. In this way, independent measurements of tracking accuracy can be provided and translated to other applications. Another limitation is the use of a single tracked tool to acquire evaluation data [7]. Some studies have demonstrated the dependency of the tracking accuracy on the geometric design of the rigid-body. A non-optimal design could lead to amplification of the *tracking error* and therefore, bias the assessment [3], [7], [30]–[32]. In addition, not all studies consider the well-described spatial dependency of the accuracy inside the working volume. Some authors provide the tracker accuracy in terms of the target-to-cameras distance to overcome this limitation [40]. However, this methodology is no longer persuasive since the spatial arrangement of cameras is flexible and such distances are not constant when using a multicamera tracker. Other studies use coordinate measurement machines or linear testing apparatus to evaluate the volumetric accuracy of trackers [4], [8], [25], [32]. In those cases, a registration process is needed to provide an absolute accuracy measurement, and this may also bias the assessment.

A major source of concern when assessing a multicamera tracker system is the problem of occlusions and its consequences for the tracking accuracy. When the line-of-sight is compromised for one or more cameras, multicamera trackers are still able to track the objects due to the data redundancy provided by the remaining non-occluded cameras [41], [42]. Hence, it is very important to consider the dependency of accuracy on the number of occluded cameras to ensure a fair assessment.

Finally, calibration is an important aspect when evaluating a tracking system with several cameras. Tracking accuracy depends on the quality of calibration. Commercial trackers (two-cameras) are commonly calibrated *a priori* by the manufacturer since camera location is fixed. However, multicamera optical trackers must be calibrated *in situ*. This step is time-consuming and must be carried out under designed conditions: a clear working volume, specific calibration tools and finely tuned camera parameters (illumination, threshold and exposure). If a single camera miscalibration occurs after initial calibration, the *tracking error* induced by this camera could be compensated by the remaining (well-calibrated) cameras. However, this condition might lead to a loss of accuracy that could be prevented if a calibration assessment is periodically and pre-operatively performed [27]. Nevertheless, there is no established protocol to control the reliability of the calibration for multicamera optical trackers. Therefore, the assessment of this kind of tracker for IGS applications should include a study of the accuracy dependence on miscalibration.

The number of image-guided applications using OptiTrack is increasing because of the above-mentioned advantages. Nonetheless, to the best of our knowledge, the available literature [24], [25] contains no extensive studies of the system that validate accuracy in terms of camera occlusions, miscalibrations, tracked tools used or against a persuasive gold standard with significantly higher accuracy.

The purpose of this study was to evaluate an OptiTrack multicamera optical tracker in terms of accuracy, sensitivity to miscalibration, camera occlusions and detection of tools for IGS applications using a feasible clinical setup. The tracker was installed in a clinical OR and an accuracy assessment was performed using a robotic arm ($\sim\mu m$ precision) as the gold standard, a single reflective marker and various tracked objects (rigid bodies).

II. MATERIAL AND METHODS

A. OPTICAL TRACKER

The tracker we evaluated consists of a set of 8 OptiTrack Flex13 cameras (1280 x 1024 image resolution, 4.8 x 4.8 µm pixel size and a frame rate in the range of 30-120 frames per second). Each camera has a 5.5-mm F#1.8 lens and an 800-nm infrared (IR) long pass filter with a horizontal and vertical field of view (FOV) of 56 and 46 degrees, respectively. Flex13 cameras illuminate the scene with a light-emitting diode (LED) ring composed of 28 LEDs (850 nm) with adjustable brightness (Fig. 2, a). Cameras are arranged around the working volume and connected to a USB hub which is controlled using the manufacturer' software.

The number and position of the cameras are selected by the user depending on the application requirements. In our case, large working volume, high accuracy and robustness against occlusions are mandatory requirements for the location of the IOERT radiation collimator. Eight Flex13 cameras were installed in the IOERT operating room at the Hospital Gregorio Marañón (Madrid, Spain) to cover the large working volume that includes the surgical table. This setup (hereinafter referred to as 'OR scenario', Fig. 3) allows surgeons to navigate procedures for different anatomical targets without modifying the cameras' spatial configuration.

Several reflective marker diameter sizes are offered by the manufacturer depending on the specific application (Fig. 2, c). In the present study, we used an 11.5-mm diameter marker from NaturalPoint (7/16'' hard model [16]) for all experimental setups since it is the manufacturer's recommended size for the OR tracking volume studied.

The calibration of this system requires a specially designed tool (Optiwand, Fig. 2, d), which is provided by the manufacturer. This tool consists of three aligned markers with known fixed positions. The calibration procedure starts by moving the calibration tool along the working volume. Since the system knows the spatial configuration of the calibration tool's markers, relative positions of the cameras can be computed by using the projections of the markers for several acquired spatial locations of this rigid body. These samples should be acquired over the whole working volume, and their number will determine the quality and accuracy of

the calibration. When sufficient samples have been acquired, the manufacturer' software estimates the best calibration parameters from the available set of calibration samples in a least-squares sense. For all experiments in this work, we calibrated the system following the manufacturer's instructions (~3000 projection samples of the calibration tool for each used camera).

B. SYSTEM ACCURACY ASSESSMENT

We designed a second scenario (hereinafter referred as the 'robotic scenario', Fig. 4) to determine the true accuracy of the 8-camera system installed in the OR. To provide a proper gold standard, we used an ABB IRB 1600 industrial robotic arm (ABB Inc., Zürich, Switzerland) whose accuracy is one order of magnitude higher than the optical tracker accuracy assessed (submillimeter, as specified by the manufacturer). The robot has a position repeatability error of 0.02 mm and a 1.2 m reachability which is able to cover the OR working volume (Fig. 4, a1).

To simulate the OR cameras arrangement (Fig. 3, a) on the robotic scenario (Fig. 4) we built a metallic structure (Fig. 4, a2 & b) which was used to mount the 8 cameras over the robot reaching volume (Fig. 4, a3). Then we performed two experiments to study the accuracy of the system under occlusions using a single reflective marker (*Study of the accuracy and occlusions,* Sec. II.B.1) and using different tools (rigid-bodies) (*Study of the accuracy of tools*, Sec. II.B.2).

1) STUDY OF THE ACCURACY AND OCCLUSIONS

We attached a single marker to the robot tip which was moved inside the working volume along a 50 mm (g_t) step path (Fig. 4, c). On each position, the location ($\overline{\boldsymbol{p}}_k$) of the marker was estimated using the optical tracker as the mean value of 1000 acquired samples ($N_{samples}$).

To determine the accuracy, we compared the position of the marker provided by the optical tracker ($\overline{\boldsymbol{p}}_k$) and the robot ($\boldsymbol{r}_k$). However, a straightforward comparison is not possible, since the geometrical spaces of the tracker and robot do not match. A possible solution could be the registration of both point-sets corresponding to each coordinate space. However, this strategy could bias the evaluation due to registration errors. Instead, we computed the distances of each studied position to its neighbors and calculated the root mean squared distance as (1):

$$d(\overline{\boldsymbol{p}})_{rms} = \sqrt{\frac{1}{N_{neighbors}}\sum_{j}^{N_{neighbors}}\left\|\overline{\boldsymbol{p}} - \boldsymbol{n}_j(\overline{\boldsymbol{p}})\right\|^2} \qquad (1)$$

where $\overline{\boldsymbol{p}}$ is the mean position provided by the tracker of the point $\boldsymbol{p}$, $N_{neighbors}$ the number of closest neighbors and $\boldsymbol{n}_j(\overline{\boldsymbol{p}})$ is the position of the j-th neighbor of the point $\boldsymbol{p}$. Each measured point has six neighbors ($N_{neighbors} = 6$) if it is inside the working volume studied (Fig. 4, c), while points placed at the corners and sides show three and four neighbors, respectively.

Ideally this distance ($d(\overline{\boldsymbol{p}})_{rms}$) would be equal to the programmed robot step size ($\|d(\overline{\boldsymbol{p}})_{rms} - g_t\| = 0$), but this is not true due to the limited accuracy of the optical tracker. We estimated the tracking error at point $\boldsymbol{p}$ ($\widehat{TE}(\boldsymbol{p})$) as this difference (2):

$$\widehat{TE}(\boldsymbol{p}) = \sqrt{\frac{1}{M}\sum_{k}^{M}\|d(\overline{\boldsymbol{p}}_k)_{rms} - g_t\|_k^2} \qquad (2)$$

where $\widehat{TE}(\boldsymbol{p})$ is the estimated tracking error at studied point $\boldsymbol{p}$, $g_t = 50\ mm$ is the robot step size and M is the number of experiment repetitions.

We measured the $\widehat{TE}$ (2) on each point of the working volume ($M = 10$ repetitions) for the calibrated system and in different occlusion scenarios: 1, 2, 3, 4 and 5 occluded cameras. We covered the camera lens with an opaque coating to simulate occlusions, performing $M = 10$ repetitions when occluding a single camera. For the remaining cases studied (2, 3, 4 and 5 occluded cameras), we were unable to run all possible (210) occlusion scenarios because of time limitations. Instead, we randomly chose the occluded camera group. For each number of occluded cameras, we performed $M = 15$ acquisitions avoiding occluded group repetition and estimated the *tracking error* ($\widehat{TE}$) following (2). Finally, we performed an Analysis of Variance (one-way repeated measures ANOVA) analysis of the *tracking error* for the different occlusion scenes.

2) STUDY OF THE ACCURACY OF TOOLS

To complete the system accuracy study, we measured the *tracking error* (2) attaching different rigid bodies to the robot tip in the occlusion-free setup. We estimated the *tracking error* (2) at the tool's pivot point (point P in Fig. 5) for four different tools: an in-house pointer with six markers (BiiG Pointer, Fig. 6, a), the NDI Polaris pointer (four markers, Fig. 5, c), a configurable rigid body (OptiTrack, four markers, Fig. 5, d) and an in-house tracked IOERT collimator (four markers Fig. 5, b). We performed $M = 5$ repetitions for each tool studied. The transformations relating the rigid-body and the pivot points (Fig. 5, P) were computed from the blueprints of each tool. However, note that our *tracking error* estimate (2) is independent of the pivot position when using rigid tools. We analyzed the *tracking error* of the different tools by means of an ANOVA analysis (one-way repeated measures).

C. CALIBRATION ASSESSMENT

1) MISCALIBRATION SENSITIVITY STUDY

We mounted a two-camera system in the OR scenario and attached a rotation sensor (PhidgetSpatial Precision 3/3/3, Phidgets Inc., Alberta, Canada) to the back of one camera (Fig. 6, b). This sensor has a resolution of 0.02 degrees/s in both the X and the Y axes and 0.013 degrees/s in the Z axis. Thereafter we performed the system calibration according to

the manufacturer's instructions (~3000 samples of the calibration tool position) and fixed a reflective marker in the inner part of the working volume at ~1.5 m.

We acquired $N_{cal} = 5000$ samples of the position of the marker and computed the mean marker location ($\overline{\boldsymbol{p}}_0$) using the calibrated system. Then we manually rotated the camera with the attached orientation sensor to cause a miscalibration. This manual rotation was performed on the yaw axis that rotates around the mounting screw of the camera (Fig. 6, α). Using the rotation sensor, we measured the produced rotation (α, mean value of $N_\alpha = 5000$ samples). After the first manual miscalibration, we repeated the acquisition for the position of the marker ($\overline{\boldsymbol{p}}_\alpha$). We repeated the rotations (miscalibration) until the system was unable to track the marker. In each case, we performed $M = 10$ repetitions.

We defined the *calibration error* ($\widehat{CE}$) as the difference between the calibrated ($\overline{\boldsymbol{p}}_0$, $\alpha = 0$ deg) and miscalibrated ($\overline{\boldsymbol{p}}_\alpha$) marker position (3). Moreover, we defined the miscalibration threshold as the maximum rotation value (α_{th}) before the tracker software reported no markers in the working volume. The miscalibration sensitivity of the two-camera system was evaluated in terms of the defined *calibration error* and the rotation value (α).

$$\widehat{CE}(\alpha) = \|\overline{\boldsymbol{p}}_\alpha - \overline{\boldsymbol{p}}_0\| \qquad (3)$$

We tested the relationship of the calibration error and the miscalibration rotation by means of an ANOVA test (one-way repeated measures).

2) MISCALIBRATION DETECTION PROTOCOL

Miscalibrations occur during real procedures for many different reasons. For instance, in our OR (Fig. 3) a camera could deviate from its calibrated position by surgical lamp blows (Fig. 3, c). When miscalibrations occur, multicamera optical trackers usually preserve the tracking capabilities. However, accuracy could be compromised without any warning to the user. In IGS applications, accuracy loss could lead to erroneous surgical tool guidance. Therefore, we propose a new miscalibration detection protocol and studied its feasibility.

The proposed protocol is based on the *calibration error* defined in (3). Suppose that we have a multicamera system formed by N cameras and one of them is miscalibrated. Tracking is expected to be feasible since the rest of cameras are calibrated. This tracker can be seen as a set of subsystems of two-cameras ($[i,j]$ *such as* $i \neq j;\ i \in [1,N];\ j \in [1,N]$). A higher *tracking error* is expected from the subsystems which contain the miscalibrated camera. For a single marker, the estimated position using the camera pairs that include miscalibrated cameras will differ from the position obtained using all the cameras. Therefore, these location differences may be used as a metric of miscalibration. The proposed methodology for miscalibration detection can be followed before any surgical procedure to ensure accurate guidance and has the following steps:

i. A single reflective marker is placed into the working volume. This marker must be detected by the projection plane of each camera.
ii. The marker three-dimensional position ($\overline{\mathrm{p}}_{\mathrm{All}}$) is recorded using all cameras.
iii. The marker position (4) is acquired using all possible sets of two-cameras that constitute the multicamera system:

$$\overline{\boldsymbol{p}}_{[i,j]} \quad such\ as\ i \neq j;\ i \in [1,N];\ j \in [1,N] \qquad (4)$$

iv. The three-dimensional location of the marker acquired using each camera pair is compared with the location acquired using all the cameras to estimate the *miscalibration error* ($\widehat{\mathrm{ME}}$) of each camera pair (5).

$$\widehat{ME}[i,j] = \left\|\overline{\boldsymbol{p}}_{[i,j]} - \overline{\boldsymbol{p}}_{All}\right\|, such\ as\ i \neq j;\ i \in [1,N];\ j \in [1,N] \qquad (5)$$

where $\widehat{ME}[i,j]$ is the miscalibration error of the pair composed by cameras i and j.
v. Camera pairs that are unable to track the marker or showing values of $\widehat{\mathrm{ME}}[\mathrm{i,j}]$ greater than a certain threshold will identify the miscalibrated cameras of the system.

3) FEASIBILITY STUDY OF THE MISCALIBRATION DETECTION PROTOCOL

To demonstrate the feasibility of the proposed miscalibration detection protocol, we calibrated the multicamera system installed in the OR (eight Flex13 cameras) following the manufacturer's instructions. After calibration, a reflective marker was placed in a fixed position inside the working volume of the tracker (Step 1). Then, (Step 2) we collected $N = 1000$ samples of the position provided by the calibrated 8-camera system and (Step 3) by each possible camera pair ($[i,j]$, $\binom{8}{2} = 28$ camera pairs). We manually miscalibrated (rotating around yaw axis) one, two, three and four randomly-selected cameras. In each miscalibration scenario we followed the proposed protocol and computed the miscalibration error (Step 5). In this case, a threshold value of 1.5 mm miscalibration error was used to determine the miscalibrated cameras (t-test, H_0: $\widehat{ME} < 1.5$ mm).

III. RESULTS

A. SYSTEM ACCURACY ASSESSMENT

1) STUDY OF THE ACCURACY AND OCCLUSIONS

Fig. 7 shows the tracking error ($\widehat{TE}$) within the whole working volume (300 × 500 × 400 mm) and for two smaller inner volumes (200 × 400 × 300 mm and 100 × 200 × 100 mm). We found that the tracking error increased with the number of occluded cameras ($p < 0.001$). Moreover, it can be noted that higher $\widehat{TE}$ was produced at the outer part of the working volume, since the smaller inner volumes showed lower $\widehat{TE}$. Table I summarizes the numerical results. In cases of non-occlusion, the mean $\widehat{TE}$ was 0.24 mm which is comparable to the manufacturer specifications. Table I shows how the $\widehat{TE}$ distribution is highly right-skewed and how high $\widehat{TE}$ values are likely to occur (higher values for 95 and 99 percentiles) when the number of occluded cameras increases.

2) STUDY OF ACCURACY OF THE TOOLS

Fig. 8 and Table II show the results for the tracking accuracy of the tools. Here, the tracking error $\widehat{TE}$ over the tracking volume is summarized for each tool. There is a clear constant difference between the $\widehat{TE}$ produced when using the commercial tools (Polaris pointer and Natural Point marker set) and the in-house tools ($p < 0.001$). However, the absolute difference is small, ~0.003 mm. It is also noteworthy that the tracking error $\widehat{TE}$ was dramatically smaller for rigid bodies than for a single marker (Table I). This is expected, since the location of the tools is computed from several tracked markers and the system uses the spatial configuration of the markers to compensate for single-marker tracking errors. In fact, using a 4-marker rigid body seems to reduce tracking error by an order of magnitude. This tracking error $\widehat{TE}$ is almost constant over the whole working volume (Table II), with a low spatial dependency of the tracking accuracy for all tools (Table II, third column).

B. CALIBRATION ASSESSMENT

1) MISCALIBRATION SENSITIVITY STUDY

Miscalibration sensitivity study results are summarized in Fig. 9. The 'x' axis shows the mean and standard deviation of the produced camera rotation (α, miscalibration). The 'y' axis shows the mean and standard deviation of the estimated calibration error $\widehat{CE}$, (3). Table I shows the data points of Fig. 9.

Note that when the system is calibrated ($\alpha = 0$ deg), the measured angle is null because no rotation has been made on any of the cameras. We performed four manual miscalibrations, although only three are shown in Fig 9. The last miscalibration caused OptiTrack to report no markers inside the working volume (Table III), indicating that the maximum miscalibration (i.e. α_{th}) is below ~0.2 deg rotation. According to the results, miscalibrations higher than α_{th} lead the system to report no markers inside the working volume for a two-camera setup. Furthermore, it is remarkable that the tracking error increases more than 3 mm for a rotation greater than 0.1 degrees. The estimated sensitivity was 29.92 mm/deg ($R2 = 97\%$, $CI = [0.94, 1.00]$). According to the ANOVA test there were differences ($p < 0.001$) in the calibration error for the three camera orientations.

2) FEASIBILITY STUDY OF THE MISCALIBRATON DETECTION PROTOCOL

The results of the study of the feasibility of the miscalibration detection protocol are shown in Fig. 10. For each experimental case—with a different number of miscalibrated cameras—the estimated miscalibration error $\widehat{ME}$ (5) of each camera pair is plotted. Most pairs containing a miscalibrated camera reported no tracked marker in their working volume. However, some of the miscalibrated pairs were still able to track the marker. For example, in Fig. 10 b, where camera '6' was miscalibrated, pairs 5-6 and 6-7 preserved their tracking ability but showed higher $\widehat{ME}$ (> 30 mm, $p < 0.001$). Those cases showed a miscalibration error greater than 1.5 mm and, hence, were detectable according to the proposed protocol. As for the calibrated pairs, the tracking error was noticeably smaller (depicted in blue, $p < 0.001$).

IV. DISCUSSION AND CONCLUSION

We performed an exhaustive assessment of the accuracy of the OptiTrack tracking system for IGS applications. To our knowledge, this is the first study to assess the tracking accuracy of the OptiTrack system using Flex 13 cameras. We analyzed the spatial distribution of tracking accuracy for a single marker and studied camera occlusions using a well-characterized gold standard (i.e. a robotic arm with µm accuracy). Moreover, we assessed the dependence of accuracy on different tools used during IOERT collimator guidance. Furthermore, we studied the system's sensitivity to miscalibration in terms of calibration error. Finally, we also proposed and validated a new miscalibration detection protocol in a surgical environment that can be automatically performed in an IGS navigation scenario.

The main original contribution of this study is the analysis of space-dependent accuracy in occlusions. The 8-camera spatial configuration showed a 99 percentile tracking error ($\widehat{TE}$) of 3.31 mm (Table I) and a mean value of 0.24 mm inside the whole working volume (300 × 500 × 400 mm). This value represents the pure accuracy of the system when occlusions and miscalibrations are not present. The results showed that $\widehat{TE}$ was dependent on the number of occluded cameras (Fig. 7 and Table I). We would like to point out that this trend also depends on the size of the working volume: the smaller the working volume, the lower the tracking error, even when occlusions are present. This is consistent with the working volume design, where the outer part of the volume is covered by a lower number of sensors leading to larger errors at the volume edges [7], [11]. Note that when occlusions affect the system, outer parts could be tracked by a reduced number of cameras or even not covered by any camera. In [11], the authors emphasized the importance of the spatial dependency of the accuracy, showing that the

Polaris system errors are higher at the upper right corners of its working volume and generally increase with the distance from the cameras. This effect is similarly depicted in Fig. 7 and Table I for Optitrack, where the robustness of the multicamera system is demonstrated. A percentile 75 *tracking error* was always below 0.23 mm for up to 5 occluded cameras. However, the mean rms *tracking error* values for the occluded cases showed much higher values (Table I). This means that occlusions produce a higher number of tracking error outliers instead of a significant loss of accuracy inside the working volume. Consequently, occlusions during tracking are important and should be considered when OptiTrack is used for an IGS navigation scenario. When an occlusion occurs, the multicamera system is expected to compensate by using the remaining cameras (system redundancy). In such cases, this compensation reduced the overall accuracy of the system. There is a tradeoff between the number of cameras used (spatial redundancy in occlusions) and the size of the working volume. For an application with a low risk of occlusion, the working volume could be larger for a given number of cameras. However, clinical applications that present a high risk of occlusion (such as IOERT) should reduce the working volume in favor of camera redundancy to avoid a notable loss of accuracy or increase the number of cameras used.

The use of tracked tools (rigid-bodies) demonstrated an improvement in accuracy (Fig. 8). Tracked tools reduced the *tracking error* $\widehat{TE}$ by an order of magnitude (Table II). It is also noteworthy that tracking accuracy depends on the spatial distribution of the tool's optical markers. In fact, the Polaris pointer demonstrated higher accuracy (0.0501 ± 0.0001 mm tracking error) than the IOERT applicator (0.0527 ± 0.0001 mm tracking error) or the in-house pointer (mean tracking error of 0.0593 ± 0.0338 mm). The tracking error dependency on the spatial distribution of markers has been previously assessed [31], [43], demonstrating the importance of designing optimal rigid bodies for optically tracked surgical tools. In our case, the design of the IOERT applicator and the custom pointer must be revised to ensure a fair accuracy during guidance. One possible explanation for the lower accuracy of the in-house pointer is the number of markers of the rigid body. When this number is high, the marker-to-marker distance should be higher to avoid inter-marker occlusions. Such occlusions could impede the detection of the marker by the optical sensors, thus leading to a loss of accuracy. Nevertheless, we would like to point out that the differences in the tracking accuracy of the tools are below ~0.01 mm (Table II), which is negligible for most clinical applications. In this study, all the tools were calibrated following the blueprint specifications. However, in several applications a pivoting calibration is needed. In [7], the authors assess this issue using a similar multicamera system. They demonstrate that the tool calibration improves the accuracy if the pivoting is performed at the center of the system working volume since it is tracked by the maximum number of optical sensors. This limitation does not apply to our results, since the metric used for evaluation purposes (2) does not depend on the tool calibration, so we have studied pure intrinsic accuracy of the system without registration and/or tool dependencies.

We found that the system had a miscalibration sensitivity of ~30 mm/deg and a maximum rotation threshold of 0.16 ± 0.09 degrees (Fig. 9, Table III). Our experiment confirmed the dependence of tracking accuracy on calibration quality. Even though this value was estimated from a system comprising two cameras, the reported sensitivity highlights the importance of calibration quality in an IGS scenario based on multi-camera tracking. It is also noteworthy that the sensitivity of calibration is directly proportional to the camera marker distance, since the resolution of the sensor is directly related to the *projection error* [11]. Hence, for larger working volumes (larger marker-to-sensor distances), the loss of accuracy for a constant miscalibration rotation could be larger than that reported here (Table III).

Our miscalibration detection protocol proved to be feasible for clinical use. A non-experienced user can evaluate the calibration using a single marker in the working area and detect which cameras deviate from the calibrated orientation automatically. Multicamera tracker setups are prone to miscalibration owing to factors associated with manual installation (e.g. screws and mounting) and OR factors (e.g. surgical lamps). We assumed that the tracking software (provided by the manufacturer) does not identify miscalibrations during real-time tracking. This could lead to a loss of accuracy if the information gathered from a miscalibrated camera is used to solve the three-dimensional location of a marker. Furthermore, if occlusions are present using the well-calibrated cameras, the expected loss of accuracy could be very limiting. Nevertheless, the high miscalibration sensitivity observed ensures that even very small miscalibrations (~0.16 degrees, Table III) are detectable. These results provide support for our protocol, which ensures that the IGS tracking setup is both accurate and reliable. Our protocol verifies the tracking reliability before a procedure in IGS applications and is not designed for continuous or real-time validation. Nevertheless, the user could run the proposed protocol any time, even during surgery, for tracking assessment. When a miscalibration is detected, we suggest disconnecting the miscalibrated camera if a new calibration cannot be performed (i.e. owing to surgical or time restrictions). This solution would result in a lower number of cameras; however, it would ensure that the system does not contain any miscalibrated camera that could deteriorate the accuracy expected. Naturally, when time and clinical restrictions are not limiting factors, repeating system calibration would be the better option for maintaining the maximum number of cameras and thus ensuring higher accuracy.

During the calibration assessments, we caused miscalibrations by manually rotating the cameras from their

mounting screw. In that sense, we only evaluated geometrical miscalibration along the screw direction. This is not illustrative of all the possible cases. However, it provides valuable information about the system sensitivity in a common miscalibration situation in a OR based on our experience.

Our study is limited by the spatial configuration of the cameras and the number of cameras used, which may not be suitable for other applications. We used 8 cameras surrounding the patient area as the working volume. However, given the large number of possible spatial configurations of the multicamera optical tracker, a more in-depth evaluation would prove cumbersome. A possible approach to overcome this limitation could be to perform simulations using the camera pair accuracy reported for different spatial configurations. Nonetheless, the OR setup used in this study covers a wide range of IGS applications, since it was installed in a real clinical environment and is therefore comparable to other possible scenarios. Many clinical IGS applications could benefit from this approach, since a main limitation of 2-camera optical tracking systems is the line-of-sight requirement between the tracked tool and the cameras. This requirement is reduced with our setup thanks to camera redundancy.

The initial IOERT radiation field is usually designed to include a 3 to 5 cm margin beyond the tumor bed in order to reduce the risk of metastatic spread [44]. The 8-camera setup we studied demonstrated reasonable accuracy for the positioning of the IOERT radiation collimator. The tracking error for a single marker proved to be below 0.38 mm for 99% of the positions inside the working volume (Table I). However, the accuracy results for the tools study (Table II) indicated that this error is expected to decrease when tools are used (Fig. 8). In a preliminary study, we demonstrated the feasibility of using OptiTrack (V100:R2 camera model) for applicator guidance (*tracking error* < 2 mm) during IOERT with a CT scanner as the gold standard [6]. The current study confirms and extends our preliminary results (using a newer camera model) and completes our assessment of the system.

In conclusion, the OptiTrack 8-camera optical tracker was evaluated for miscalibration sensitivity, accuracy, camera occlusions and tool detection using a feasible clinical setup. The system is accurate for IGS navigation, improves redundancy and allows for larger working volumes. Our assessment and the validated miscalibration protocol are important contributions to the IGS community, where the choice of the tracker for surgical applications is critical and knowledge of the system accuracy under situations of camera occlusion is mandatory.

ACKNOWLEDGMENT

The authors also extend their gratitude to the radiotherapy technicians at Hospital General Universitario Gregorio Marañón and to Laura Sanz for their support.

REFERENCES

[1] K. Cleary and T. M. Peters, Image-guided interventions: technology review and clinical applications, vol. 12, no. 1. Annual Reviews, 2010.
[2] T. Peters and K. Cleary, Image-guided interventions: Technology and applications. 2008.
[3] T. Haidegger, K. P, I. Rudas, B. I. Benyó, and Z. Benyó, "The Importance of Accuracy Measurement Standards for Computer-Integrated Interventional Systems," 2010.
[4] I. J. Gerard and D. L. Collins, "An analysis of tracking error in image-guided neurosurgery," Int. J. Comput. Assist. Radiol. Surg., vol. 10, no. 10, pp. 1579–1588, Oct. 2015.
[5] N. C. Atuegwu and R. L. Galloway, "Volumetric characterization of the Aurora magnetic tracker system for image-guided transorbital endoscopic procedures," *Phys. Med. Biol.*, vol. 53, no. 16, pp. 4355–4368, Aug. 2008.
[6] V. García-Vázquez, E. Marinetto, J. A. Santos-Miranda, F. A. Calvo, M. Desco, and J. Pascau, "Feasibility of integrating a multi-camera optical tracking system in intra-operative electron radiation therapy scenarios," *Phys. Med. Biol.*, vol. 58, no. 24, pp. 8769–8782, 2013.
[7] Z. Min, D. Zhu, and M. Q.-H. Meng, "Accuracy assessment of an N-ocular motion capture system for surgical tool tip tracking using pivot calibration," in *IEEE International Conference on Information and Automation (ICIA)*, 2016, pp. 1630–1634.
[8] R. Elfring, M. de la Fuente, and K. Radermacher, "Assessment of optical localizer accuracy for computer aided surgery systems," *Comput. Aided Surg.*, vol. 15, no. 1–3, pp. 1–12, Feb. 2010.
[9] R. Hartley and A. Zisserman, "Multiple View Geometry in Computer Vision," *Robotica*, vol. 23, no. 2, pp. 271–271, Mar. 2005.
[10] R. Khadem *et al.*, "Comparative tracking error analysis of five different optical tracking systems," *Comput. Aided Surg.*, vol. 5, no. 2, pp. 98–107, 2000.
[11] A. D. Wiles, D. G. Thompson, and D. D. Frantz, "Accuracy assessment and interpretation for optical tracking systems," in *International Society for optics and photonic. (SPIE) Medical Imaging 2004: Visualizations, Image-guided Procedures and Display*, 2004, vol. 5367, pp. 421–432.
[12] R. Tranberg, *PhD Thesis. Analysis of body motions based on optical markers: acuracy, error analysis and clinical applications*. 2010.
[13] T. Sielhorst, M. Bauer, O. Wenisch, G. Klinker, and N. Navab, "Online estimation of the target registration error for n-ocular optical tracking systems," *Med. Image Comput. Comput. Assist. Interv.*, vol. 10, pp. 652–659, 2007.
[14] B. Li, L. Zhang, H. Sun, J. Yuan, S. G. F. Shen, and X. Wang, "A novel method of computer aided orthognathic surgery using individual CAD/CAM templates: a combination of osteotomy and repositioning guides," *Br. J. Oral Maxillofac. Surg.*, vol. 51, no. 8, p. 239, Dec. 2013.
[15] E. Marinetto *et al.*, "Optical Tracking System Integration into IORT Treatment Planning System," in *Mediterranean Conference on Medical and Biological Engineering and Computing*, 2014, 25/09/2013., vol. 25–28 sept, pp. 37–40.
[16] "NaturalPoint, Inc. - Optical Tracking Solutions, Corvallis, OR, USA."
[17] C.-Y. Chang *et al.*, "Towards Pervasive Physical Rehabilitation Using Microsoft Kinect," in *International Conference on Pervasive Computing Technologies for Healthcare*, 2012.
[18] C. Zhu and W. Sheng, "Realtime human daily activity recognition through fusion of motion and location data," in *IEEE International Conference on Information and Automation*, 2010, pp. 846–851.
[19] B. Spanlang, J.-M. Normand, E. Giannopoulos, and M. Slater, "A first person avatar system with haptic feedback," in *ACM Symposium on Virtual Reality Software and Technology*, 2010, p. 47.
[20] D. Webster and O. Celik, "Experimental evaluation of Microsoft Kinect's accuracy and capture rate for stroke rehabilitation applications," in *IEEE Haptics Symposium, HAPTICS*, 2014, pp. 455–460.
[21] F. Ioakeimidou, A. Olwal, A. Nordberg, and H. Von Holst, "3D visualization and interaction with spatiotemporal X-ray data to minimize radiation in image-guided surgery," in *IEEE Symposium on Computer-Based Medical Systems*, 2011, pp. 1–6.
[22] E. Marinetto, "Integrating an Optical Tracking System into IOERT

Workflow," in *12th IEEE EMBS International Summer School on Biomedical Imaging*, 2016, 16/06/2016., vol. 16–24 jun.
[23] S. J. Obst, R. Newsham-West, and R. S. Barrett, "In vivo measurement of human achilles tendon morphology using freehand 3-D ultrasound," *Ultrasound Med. Biol.*, vol. 40, no. 1, pp. 62–70, Jan. 2014.
[24] B. Carse, B. Meadows, R. Bowers, and P. Rowe, "Affordable clinical gait analysis: An assessment of the marker tracking accuracy of a new low-cost optical 3D motion analysis system," *Physiotherapy*, vol. 99, no. 4, pp. 347–351, 2013.
[25] A. M. Aurand, J. S. Dufour, and W. S. Marras, "Accuracy map of an optical motion capture system with 42 or 21 cameras in a large measurement volume," *J. Biomech.*, vol. 58, pp. 237–240, Jun. 2017.
[26] E. Marinetto *et al.*, "Optical Tracking System Integration into IORT Treatment Planning System," *XIII Mediterranean Conference on Medical and Biological Engineering and Computing 2013 (MEDICON)*, vol. 25–28 sept. pp. 37–40, 2013.
[27] T. Koivukangas, J. P. Katisko, and J. P. Koivukangas, "Technical accuracy of optical and the electromagnetic tracking systems.," *Springerplus*, vol. 2, no. 1, p. 90, Dec. 2013.
[28] H. Dang, Y. Otake, S. Schafer, J. W. Stayman, G. Kleinszig, and J. H. Siewerdsen, "Robust methods for automatic image-to-world registration in cone-beam CT interventional guidance," *Med. Phys.*, vol. 39, no. 10, p. 6484, Oct. 2012.
[29] J. B. West, J. M. Fitzpatrick, S. A. Toms, C. R. Maurer, and R. J. Maciunas, "Fiducial point placement and the accuracy of point-based, rigid body registration," *Neurosurgery*, vol. 48, pp. 810-816; discussion 816-817, 2001.
[30] L. Davis, F. G. Hamza-lup, and J. P. Rolland, "A Method for Designing Marker-Based Tracking Probes College of Optics and Photonics," in *International Symposium on Mixed and Augmented Reality*, 2004, pp. 120–129.
[31] T. Pintaric and H. Kaufmann, "A rigid-body target design methodology for optical pose-tracking systems," in *ACM symposium on Virtual reality software and technology*, 2008, pp. 73–76.
[32] L. Maier-Hein, A. Franz, H.-P. Meinzer, and I. Wolf, "Comparative assessment of optical tracking systems for soft tissue navigation with fiducial needles," 2008, p. 69181Z.
[33] W. Birkfellner, F. Watzinger, F. Wanschitz, R. Ewers, and H. Bergmann, "Calibration of tracking systems in a surgical environment," *IEEE Trans. Med. Imaging*, vol. 17, no. 5, pp. 737–742, 1998.
[34] J. D. Kertis, J. M. Fritz, J. T. Long, and G. F. Harris, "Static and Dynamic Calibration of an Eight-Camera Optical System for Human Motion Analysis," *Crit. Rev. Phys. Rehabil. Med.*, vol. 22, no. 1–4, pp. 49–59, 2010.
[35] J. Kertis, *Master's Thesis: Biomechanical Evaluation of an Optical System for Quantitative Human Motion Analysis*. 2012.
[36] D. D. Frantz, A. D. Wiles, S. E. Leis, and S. R. Kirsch, "Accuracy assessment protocols for electromagnetic tracking systems," *Phys. Med. Biol.*, vol. 48, no. 14, pp. 2241–2251, Jul. 2003.
[37] J. Hummel *et al.*, "Evaluation of a new electromagnetic tracking system using a standardized assessment protocol," *Phys. Med. Biol.*, vol. 51, no. 10, pp. N205–N210, May 2006.
[38] R. Rohling, P. Munger, J. M. Hollerbach, and T. Peters, "Comparison of Relative Accuracy Between a Mechanical and an Optical Position Tracker for Image-Guided Neurosurgery," *Comput. Aided Surg.*, vol. 1, no. 1, pp. 30–34, Jan. 1995.
[39] Y. Ehara, H. Fujimoto, S. Miyazaki, M. Mochimaru, S. Tanaka, and S. Yamamoto, "Comparison of the performance of 3D camera systems II," *Gait Posture*, vol. 5, no. 3, pp. 251–255, Jun. 1997.
[40] C. NDI Inc., Waterloo, Ontario, "Polaris Specifications," 2016.
[41] J. Wang, M. Q.-H. Meng, and H. Ren, "Towards Occlusion-Free Surgical Instrument Tracking: A Modular Monocular Approach and an Agile Calibration Method," *IEEE Trans. Autom. Sci. Eng.*, vol. 12, no. 2, pp. 588–595, Apr. 2015.
[42] J. H. Pfeiffer, Á. Borbáth, C. Dietz, and T. C. Lueth, "A new module combining two tracking cameras to expand the workspace of surgical navigation systems," in *SII 2016 - 2016 IEEE/SICE International Symposium on System Integration*, 2017, pp. 477–482.
[43] J. B. West and C. R. Maurer, "Designing Optically Tracked Instruments for Image-Guided Surgery," *IEEE Trans. Med. Imaging*, vol. 23, no. 5, pp. 533–545, May 2004.
[44] F. A. Calvo, R. M. Meirino, and R. Orecchia, "Intraoperative radiation therapy first part: rationale and techniques," *Crit. Rev. Oncol. Hematol.*, vol. 59, no. 2, p. 106, Aug. 2006.

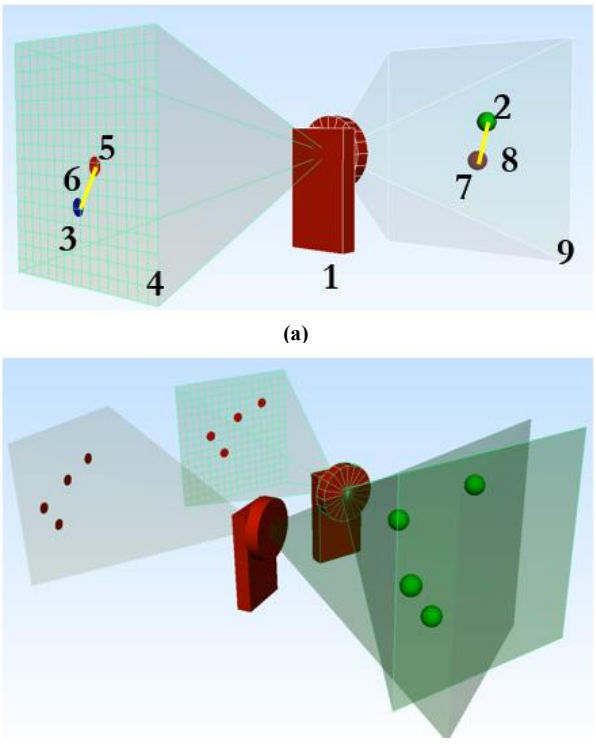

FIGURE 1. (a) Tracking error definitions. (a1) Optical tracking camera, (a2) reflective marker true position, (a3) true projection on (a4) camera plane, (a5) expected projection from calibration, (a6) camera projection error, (a7) marker location estimate, (a8) marker tracking error within (a9) camera acquisition range. (b) Two cameras imaging 4 retro-reflective targets. Target locations are determined from a forward projection of the target images on the camera image plane. Targets lie at the intersection of the projected rays.

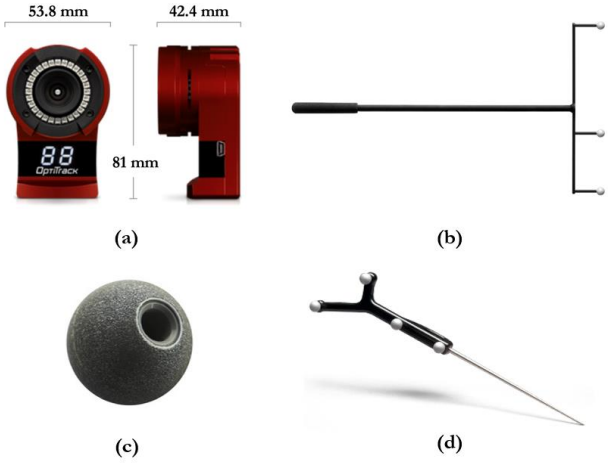

FIGURE 2. (a) OptiTrack Flex13 camera (b) Optiwand calibration tool (c) Reflective marker of 11.5 mm radius. (d) Rigid-body pointer tool (NDI, Ontario, Canada).

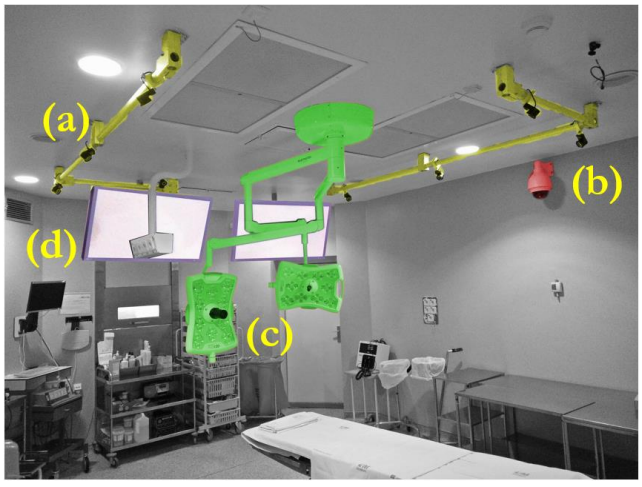

FIGURE 3. OR scenario: Distribution of cameras in Hospital Gregorio Marañón (Madrid) used for navigation of the IOERT applicator. (a) Tracker structure with 8 Flex13 cameras. (b) Video camera. (c) Surgical lights. (d) Navigation screens.

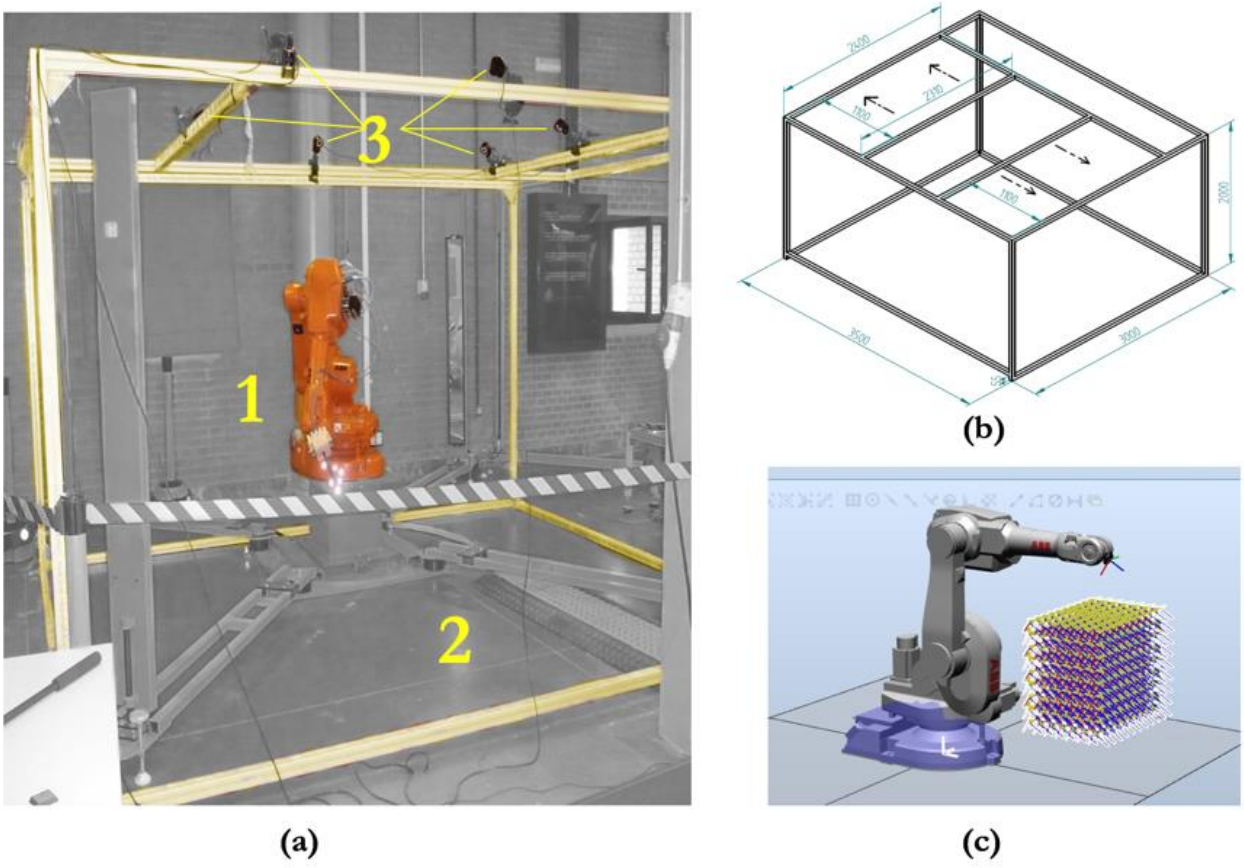

FIGURE 4. Robotic scenario (a) Experimental setup for optical tracker accuracy assessment. (a1) ABB Robot, (a2) metallic structure simulating OR camera holders, (a3) OptiTrack Flex 13 cameras. (b) Metallic structure diagram (all measurements are in mm; arrows mean that the piece is movable). (c) Programmed robot path over the working volume.

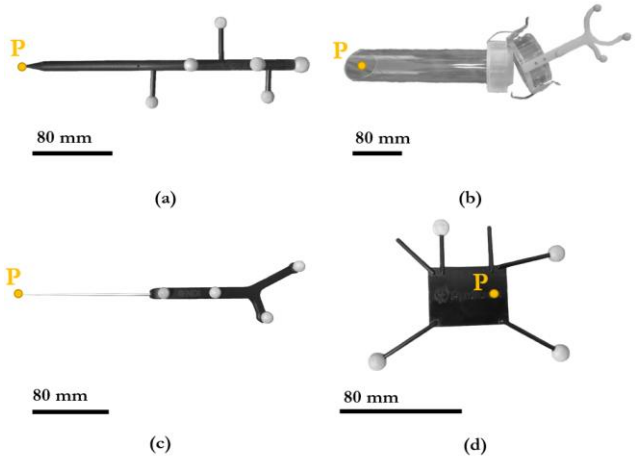

FIGURE 5. Rigid-body tools. (a) BiiG pointer. (b) IOERT applicator tool. (c) NDI Polaris Pointer. (d) NaturalPoint Marker Set: 14 mm X-Base. (P) Tracked pivot point.

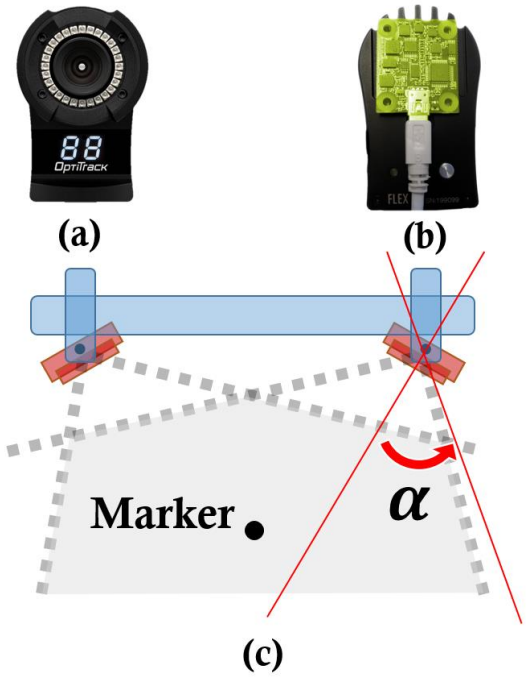

FIGURE 6. Phidget orientation sensor attached to an OptiTrack camera. (a) Front part of OptiTrack Flex 13 camera. (b) Phidget 3/3/3 attached to the camera back. (c) Experimental setup showing the marker and the produced miscalibration angle (α) in the yaw axis.

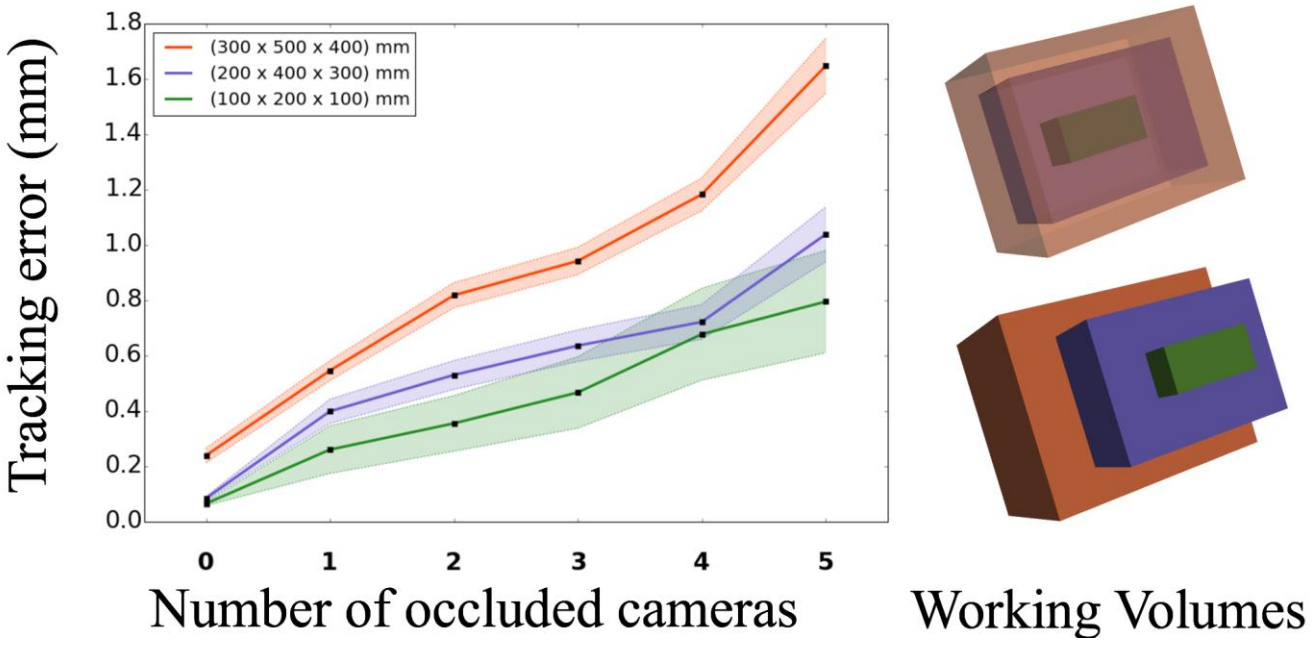

FIGURE 7. Tracking error (mean and 95% confidence interval) within the studied working volume for different numbers of occluded cameras and different inner volumes.

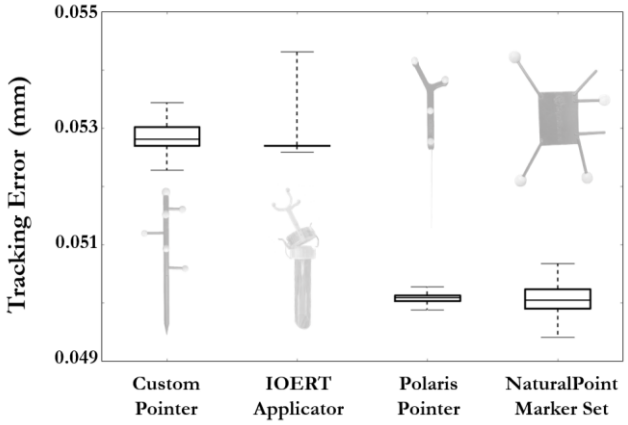

FIGURE 8. Tracking error on the working volume for different tracking tools.

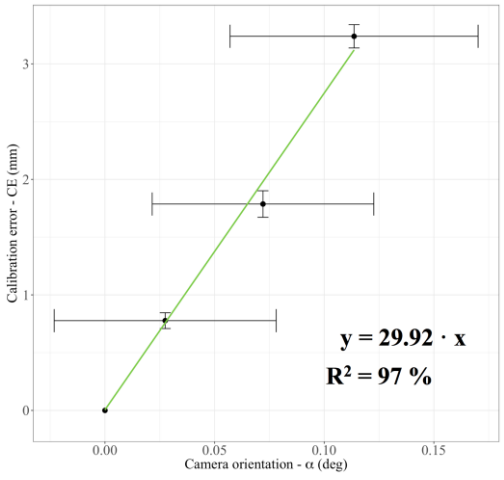

FIGURE 9. Calibration error (mean and standard deviation for the 10 repetitions) for 4 different orientations (mean and standard deviation for the 10 repetitions) of a miscalibrated camera using a 2-camera OptiTrack tracker. Sensitivity: 29.92 mm/deg (R2 = 97%, CI = [0.94,1.00]). Green line: estimated linear model of the data.

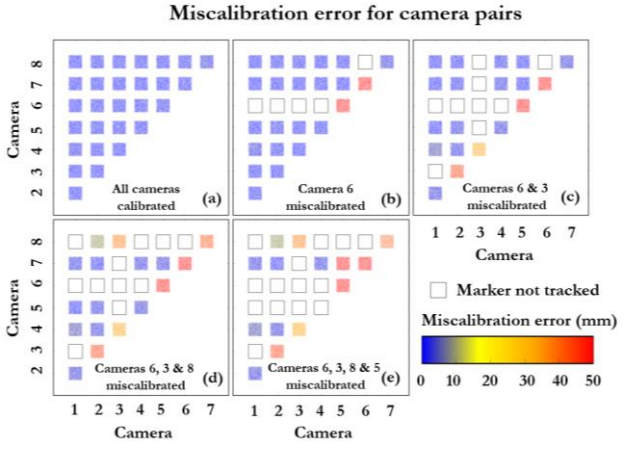

FIGURE 10. Difference in 3D position of the marker with respect to the initial reference location for different numbers of miscalibrated cameras. (a) All cameras calibrated. (b) Camera number 6 miscalibrated. (c) Cameras 6 and 3 miscalibrated. (d) Cameras 6, 3 and 8 miscalibrated. (e) Cameras 6, 3, 8 and 5 miscalibrated.

TABLE I
OCCLUSION STUDY RESULTS

Number of Occluded Cameras	Tracking Error (mm)						
	Central Statistics			Percentiles			
	Mean	Standard Deviation	Mean rms	50	75	95	99
5	1.65	5.07	5.33	0.11	0.23	10.32	22.96
4	1.18	2.99	3.21	0.12	0.24	8.52	12.73
3	0.94	2.49	2.66	0.11	0.20	8.43	12.09
2	0.82	2.31	2.45	0.10	0.18	8.39	10.64
1	0.55	1.84	1.92	0.10	0.16	3.44	9.58
0	0.24	1.05	1.08	0.08	0.13	0.38	3.31

TABLE II
TOOL TRACKING ACCURACY RESULTS

Tool	Tracking Error (mm) [mean ± std]	Tracking Error (mm) [min, max]
Custom Pointer	0.0593 ± 0.0338	[0.0523, 0.3936]
IOERT Applicator	0.0527 ± 0.0001	[0.0526, 0.0543]
Polaris pointer tip	0.0501 ± 0.0001	[0.0497, 0.0506]
NaturalPoint Marker Set	0.0501 ± 0.0003	[0.0494, 0.0510]

TABLE III
MISCALIBRATION SENSITIVITY RESULTS

Miscalibration setup	Tracked Marker	Tracking error (mm) [mean ± std]	Camera orientation (deg) [mean ± std]
First	Yes	0.78 ± 0.07	0.03 ± 0.09
Second	Yes	1.79 ± 0.11	0.07 ± 0.09
Third	Yes	3.24 ± 0.10	0.11 ± 0.10
Forth	No	-	0.16 ± 0.09